Time-Resolved Operando Analysis of the Pyrolysis of a PECVD-Deposited Siloxane Polymer Using a Combined DRIFTS-MS System

Bryan Nguyen, Farnaz Tabarkhoon, Linghao Zhao, Ankit Mishra, Malancha Gupta, Priya Vashishta, Theodore Tsotsis *

Mork Family Department of Chemical Engineering and Materials Science, University of Southern California, 925 Bloom Walk, Los Angeles, California 90089, United States

*Corresponding Author Email: tsotsis@usc.edu

Highlights:

- pV4D4 were deposited onto various substrates via the PECVD method.
- Study the mechanism of conversion of films into silica ceramics during pyrolysis reaction.
- Investigation of the impact of preparation conditions on the final structure of ceramics.
- Combination of experimental and molecular modeling to understand the pyrolysis process.

Abstract

Silicon-type thin films, made of silica, silicon carbide (SiC), or oxycarbide, find use as membranes and electronic sensors, and in semiconductor and solar energy applications. Previously, we studied[1] the preparation of nanoporous silica membranes via deposition of poly(1,3,5,7-tetravinyl-1,3,5,7-tetramethylcyclotetrasiloxane) (pV4D4) films onto SiC macroporous substrates via initiated chemical vapor deposition (iCVD) and their subsequent controlled-atmosphere pyrolysis. Here, we utilize a different method, plasma-enhanced chemical vapor deposition (PECVD), to deposit thin pV4D4 films onto a variety of substrates at significantly higher deposition rates than iCVD and employ a number of experimental techniques to comprehensively investigate the mechanism of conversion of these films into silica ceramics via

controlled-atmosphere pyrolysis. The aim of these studies is to better understand the impact of preparation conditions on the structure and properties of the resulting ceramic films. The experiments are coupled with complementary molecular simulations of the pyrolysis process that employ a reactive force field (ReaxFF). This has allowed better understanding, at the molecular level, of the processes that take place during the conversion, via pyrolysis, of the pV4D4 polymer into a silica ceramic.

Keywords: Membranes, Chemical Vapor Deposition, Silica, PECVD, pV4D4

1. Introduction

Silicon-based thin films, such as silica and silicon carbide (SiC), and oxycarbide, are useful in a variety of applications due to their versatile physicochemical properties, chemical and thermal stability, and structural stability.[2,3,4] These organosilicon thin films have been used as di-electric materials[5,6,7], anti-reflective coatings[8,9], anti-fouling layers[10,11], and in molecular separations[12,13], amongst other applications. There are several different techniques for depositing such films on substrates, including spin-coating[14], dip-coating [15,16], and chemical vapor deposition (CVD)[17,18]. CVD, in particular, allows the application of these films with conformal coverage on complex substrate surfaces[19] and without the use of toxic solvents[20,21,22].

Among the different CVD methods, plasma-enhanced chemical vapor deposition (PECVD) is an appealing choice for a variety of applications. In PECVD, a power source (AC or DC) is used to generate free radicals in a plasma atmosphere, which then react with precursor gas molecules to grow a film on a substrate surface. [23] Compared to conventional CVD, PECVD utilizes lower deposition temperatures and offers relatively high deposition rates.[24] Previously, we deposited via initiated chemical vapor deposition (iCVD) a siloxane-type polymer, poly(tetra-vinyl-tetra-methyl cyclotetrasiloxane) (pV4D4), onto a SiC porous support and pyrolyzed it in an inert atmosphere to prepare a silica thin membrane film.[1] pV4D4 is a versatile polymer that can be utilized in various applications, including in the biomedical device[25] and dielectric materials[26]

fields. In this paper, we use, instead, low-energy PECVD to deposit the pV4D4 polymer onto a variety of substrates, including silicon (Si) wafers and barium fluoride (BaF_2) powder, and study its pyrolysis to produce silica films.

There are a number of monomer precursors that produce organosilicon-type polymers which upon pyrolysis generate silicon-based ceramics. The monomer choice significantly impacts the deposition rate and the properties of the resulting polymer. V4D4, the monomer chosen in this study, is not as volatile as some of the more commonly utilized monomers for the preparation of organosilicon films (e.g., HMDSO), but its volatility is sufficiently high for it to be used in PECVD, while the presence of pendant unsaturated functional groups in its structure, i.e., four vinyl bands, result in relatively fast rates even during operation under low plasma power. Further, these pendant vinyl groups function as potential crosslinking reaction sites during polymerization. A highly crosslinked organosilicon polymer structure is highly desirable in order to produce Si-based ceramics, at high yield, via high temperature pyrolysis.

We analyze the changes in chemical structure of the pV4D4 film during pyrolysis employing a time-resolved, operando combined Diffuse Reflectance Infrared Fourier Transform Spectroscopy (DRIFTS) and Mass Spectrometry (MS) system. We combine the DRIFTS-MS investigations with parallel thermogravimetric analysis (TGA) studies of the pyrolysis process, together with Energy-dispersive X-Ray Spectroscopy (EDS) analysis of the resulting pyrolyzed materials. Furthermore, we complement the experimental studies with molecular simulations of the polymer pyrolysis process to help gain better fundamental insight into the phenomena that take place during the conversion of the polymer into a ceramic.

DRIFTS is a powerful technique that allows one to study in situ changes in the bonding environment of the polymer structure as it is being pyrolyzed.[27] Combining the DRIFTS system with a MS analyzer (also known as residual gas analyzer (RGA)) allows one to analyze the various stable gas species emitted from the polymer as it is being pyrolyzed, while simultaneously monitoring changes in its solid-state chemical composition and structure.[28] Operando DRIFTS-MS systems have been used to study catalytic reactions. Wang et al., for example, studied the kinetics of the CO_2 methanation reaction over Ru/Al_2O_3 catalysts using such a system.[29] Ochoa et al. used the technique to study the oxidation of ethanol over mixed oxide catalysts to help elucidate the different reaction pathways.[30] In the polymer pyrolysis technical area, White[31] used

a combined DRIFTS-MS system to study the thermal decomposition of polystyrene, finding that it decomposed shortly after 500 °C, but we know of no prior study of the pyrolysis of siloxane-type polymers to form inorganic materials. pV4D4 is an ideal model system for such a study, as it has a highly crosslinked siloxane structure and studying its pyrolysis could yield interesting insight into siloxane chemistry. Increasing the cross-linking in the precursor polymer has been shown to increase the ceramic yield during film pyrolysis.[32]

In this study, we combine the experimental studies of pV4D4 pyrolysis with a complementary computational analysis with the aim to gain information, at the atomistic level, that is difficult to acquire experimentally under real-world conditions. In our efforts, we utilize a reactive molecular dynamics (RMD) approach that allows large-scale simulations of chemical events, like polymer pyrolysis, at a fraction of the computational cost of QM methods.[33] We employ ReaxFF, a popular reactive forcefield that is compatible with several different software packages, including LAAMPS. In ReaxFF, interatomic distance is used to describe bond order formalism, which can then be used to predict the breaking of bonds that are present and the formation of new ones[34], thus helping bridge the gap between QC methods and empirical force-fields by simplifying the former. Our group has previously used ReaxFF to study the pyrolysis of allyl-hydridopolycarbosilane (AHPCS) into SiC.[35] Chenoweth et al.[36] modeled the pyrolysis of polydimethylsiloxane (PDMS) and found that at lower pyrolysis temperatures (up to 900 K), it depolymerized and formed cyclosiloxane oligomers. Similarly, Chen et al.[37] studied the decomposition of hexamethyldisiloxane into smaller chemical moieties, finding that the scission of Si-C bonds preceded the defragmentation of C-H and Si-O bonds, and that the main products of this pyrolysis were methane (CH_4) and linear siloxanes.

In summary, this paper introduces a methodology that can elucidate the reaction mechanism of polymer pyrolysis by combining observations of the solid-state bond changes in the polymer, evolved gas phase species analysis, and RMD molecular simulations. Having better fundamental understanding of the molecular events that take place during pre-ceramic polymer pyrolysis can help reveal how parameters such as monomer selection and the experimental conditions, including the heating rate and temperature of pyrolysis, affect the final ceramic structure and properties. This, in turn, can help experimentalists optimize monomer selection and

experimental pyrolysis protocols programs and, in the long-term, reduce energy costs during scale-up operations for inorganic materials preparations.

2. Experimental

2.1 Deposition Method

The PECVD deposition was performed inside a custom-made, pancake-shaped vacuum reactor (48 mm in height, 250 mm in diameter, GVD Corporation) with a thermally-cooled stage. The 1,3,5,7-tetravinyl-1,3,5,7-tetramethylcyclotetrasiloxane (V4D4) (Gelest, Inc., used as received without further purification) monomer was loaded into a stainless-steel jar that was held under vacuum and heated to 50 °C. The line connecting the monomer jar to the reactor was heated to 65 °C in order to prevent any adsorption or condensation of the monomer in the line. The substrates were placed on the stage of the reactor and kept at a temperature of 50 °C via a recirculating chiller (Thermo Scientific Haake A25). The V4D4 flow rate was kept constant at 1.2 sccm using a needle valve, and the nitrogen (N_2) gas flow rate into the reactor was kept constant at 40 sccm via a mass flow controller (MFC, MKS Type 1479A). A rotary vane vacuum pump (Edwards E2M40) was employed to keep the reactor under vacuum condition, at 185 mTorr, via a throttle-valve (MKS 153D) by active feedback control from a capacitance manometer (MKS 622C01TDE Baratron). An external radio-frequency (RF) plasma generator (Diener, 13.56 MHz, 100 W) was connected to a nichrome filament array (Omega Engineering, 80%/20% Ni/Cr) to ignite the plasma in order to deposit the polymer film. The power supply (25 W), monomer flow rate (1.2 sccm), and other PECVD reactor conditions were kept constant in order to maintain a continuous, steady deposition rate of ~100 nm/min.. Si wafers (Wafer World, 100 mm) were thoroughly cleaned with solvents and dried in air before being placed onto the reactor stage. In order to monitor the thickness of the pV4D4 film in-situ, a helium-neon laser interferometer (Industrial Fiber Optics) was used on a Si wafer. For the DRIFTS and TGA experiments, PECVD was used to deposit 10 μm of pV4D4 onto BaF_2 (Alfa Aesar, 40 mesh) powder. Prior to the deposition, the BaF_2 powder was dried in an oven at 100 °C for 1 h in order to remove any remaining moisture, and then it was evenly distributed on a Si wafer using a clean razor blade.

2.2 Ex-situ FTIR Analysis

pV4D4-coated Si wafers (see Sect. 2.1) were placed in the center of a tube-furnace (Lindberg/Blue, Model STF55433C). The furnace was then purged with ultra-high purity (UHP) argon (Ar) at 300 sccm for approximately 1 h, and the samples were then heated, at a heating rate of 3 °C/min, to the desired pyrolysis temperature where they were held for a 2 h hour "soak" period before being cooled down to ambient room temperature at a rate of 3 °C/min. Transmission IR spectra of both the as deposited as well as the pyrolyzed films on the wafers were collected using Fourier transform infrared (FTIR) spectroscopy (Nicolet iS10, Thermo Scientific), with a clean bare Si wafer used as the background. To collect the monomer spectra, a drop of V4D4 was placed in between two Si wafers and the spectra were collected, with two Si wafers being used as the background. The SpectraGryph-1.2 software was utilized to analyze the FTIR (and also the DRIFTS, see Sect. 2.3) spectra.

2.3 DRIFTS-RGA

The changes in the bonding environment of the polymer film were studied in-situ using DRIFTS (COLLECTOR II, Thermo Scientific). The purge line for the DRIFTS cell was connected to a mass analyzer (RGA200, Stanford Research Systems) in order to analyze the composition of gas components inside the DRIFTS chamber. The pressure of the vent line and the amount of gas entering the RGA were controlled using a series of needle valves. The apparatus is shown in Figure 1. The polymer-coated powder was placed inside the DRIFTS sample cup and was leveled using a razor blade, as recommended by the instrument manual. Ar gas with a constant flow rate of 10 sccm was then introduced into the cell to purge the chamber for approximately 1 h to remove any residual air remaining in the system. Prior to taking measurements, the RGA was allowed to reach a stable baseline. The sample in the DRIFTS cell was heated at a rate of 20 °C/min to 900 °C, and the IR absorbance spectrum was recorded at every 100 °C interval. During the experiment, the pressure of the purge line from the DRIFTS cell was kept at a minimum of 0.1 psig in order to induce a positive pressure and to ensure that ambient air did not enter through the vent lines.

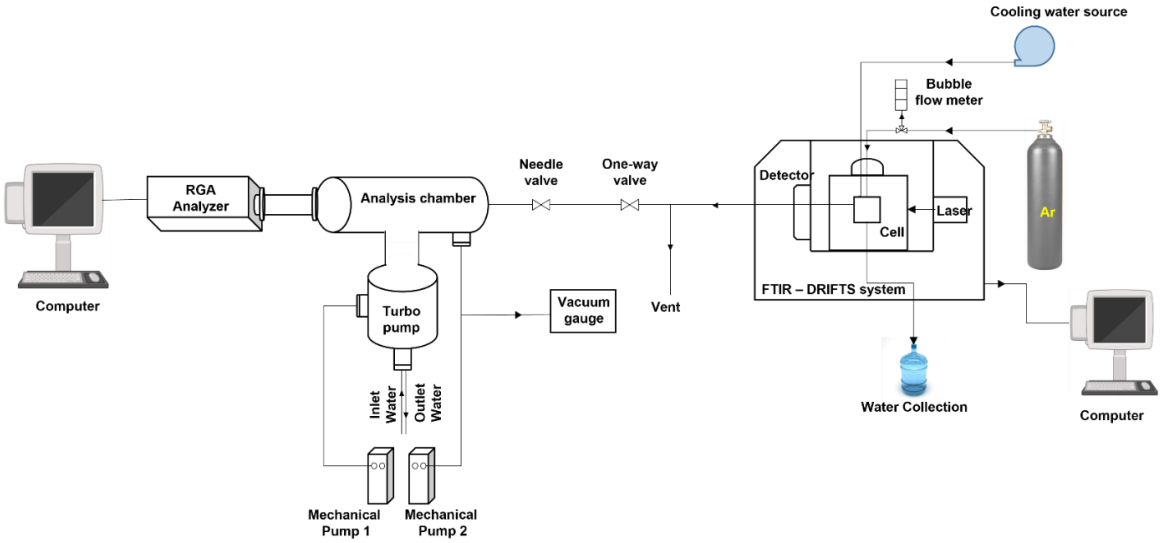

Figure 1: Schematic of the combined DRIFTS-RGA apparatus

2.4 Thermogravimetric Analysis (TGA)

Thermogravimetric analysis (Cahn Instruments, 12130-01) was used to measure in-situ the mass loss of the pV4D4 polymer during pyrolysis. For that, approximately 100 mg of the pV4D4-coated BaF_2 powder (prepared as described above in Section 2.1) was placed inside the TGA sample cup, and high-purity Ar gas was then allowed to purge the system at a flow rate of 30 sccm for 20 min. For the TGA test, the chamber was heated to 100 °C at a heating rate of 3 °C/min and held at that temperature for 2 h in order to move any residual moisture. The sample was then heated to 900 °C at a heating rate of 3 °C/min before being cooled down to room temperature at a rate 5 °C/min.

2.5 X-ray Energy Dispersive Spectroscopy (*EDS)*

A plasma focused ion beam (PFIB)/scanning electron microscopy (SEM) system (Thermo Scientific, Helios G4 PFIB UXe DualBeam FIB/SEM) with an attached x-ray energy dispersive spectroscopy (EDS) accessory was used to investigate the atomic composition of the polymer films. Data were collected with a voltage of 5 kV and a 1.6 nA beam current. The working distance of the EDS detector was set to 5.5 mm and 1,000,000 counts were collected for each sample.

3. ReaxFF Algorithm/Work-Flow

The PV4D4 system was created through open source IQMol Software and relaxed using the Universal Forcefield (UFF) available within the IQMol package.[38] We randomly reacted the vinyl bonds in a head-to-tail polymerization so that approximately 52% of the vinyl bonds were reacted for the system. The cross-linked structure, thus created, was repeated periodically to yield a system with approximately 2000 atoms. The polymer system was first initiated with 3 pV4D4 complexes of 15 monomers each, which each had the requisite vinyl reactivity. The system was then compressed using NVT-MD to a density of 1.22 gm/cc. The compressed system, thus obtained, was pyrolyzed using NVT-MD at a timestep of 0.1 fs per step at various temperatures from 300 K to 2500 K. The heating rates for the pyrolysis process were 1 K/ps, 2 K/ps and 3 K/ps. We dumped the files every 1 ps and observed the fragments formed at the given step using depth first search analysis on the molecular graph formed using the nearest bonded neighbor cutoff criteria for various atoms.

4. Results and Discussion

4.1 pV4D4 Deposition via PECVD and Ex-situ Pyrolysis as Studied by Transmission FTIR

We have found that PECVD deposits pV4D4 films at a much higher deposition rate than what was previously attained with iCVD (~100 nm/min vs. ~10 nm/min) under comparable reactor conditions. This has benefits in terms of shortening the deposition time, and thus the costs, for the preparation of these films for potential commercial uses, but also makes it more convenient to grow thicker polymeric films on substrates to test and experiment with techniques such as DRIFTS, TGA, and RGA, thus improving analytical accuracy.

Table 1. IR bands shown in Figures 2-4

Regions	**IR Bands Corresponding to Bonds**
i	C-H stretching from polyethylene bonds, asymmetric CH_3 stretching
ii	Modes related to vinyl bonds
iii	Si-CH_3 bending
iv	Si-O-Si bonding environments
v	Si-C stretching, rocking in Si-CH_3
vi	Si-O-Si out of plane deformations

Figure 2 shows the transmission FTIR spectrum of the pV4D4 polymer deposited, via PECVD, on a Si wafer. For comparison in the same Figure, we also show the FTIR spectra of the V4D4 monomer. For easy reference, Table 1 shows the various bands and their assignments to functional groups observed. There are several prominent bands which are present both in the V4D4 monomer and the pV4D4 polymer. These include bands in the region between 1000 and 1100 cm^{-1}, where one finds a broad band corresponding to the Si-O-Si bending (~1060 cm^{-1}) and the Si-O ring stretching (~1065 cm^{-1}) bands (region iv). In addition, there are several bands corresponding to the Si-C bond in both the V4D4 and pV4D4: Si-CH_3 bending (~1250-1270 cm^{-1}) (region iii), Si-C asymmetric rocking (~790 cm^{-1}) (region v), and Si-C rocking (~750 cm^{-1}) (region v).[39] There is also a sharp peak at 2960 cm^{-1} which corresponds to asymmetric CH_3 stretching in Si-CH_3. There are several bands, however, in the monomer spectrum corresponding to the vinyl bonds (peaks ii) that are not present in the polymer spectrum. They include the bands at ~960 and ~1400 cm^{-1} corresponding to the wagging and bending modes of CH_2, and the band at ~1600 cm^{-1} corresponding to the C=C stretching in vinyl bonds.[40] In addition, there is a small band at ~3060 cm-1 associated with C-H stretching in CH=C in vinyl groups.[41] These bands corresponding to the vinyl bonds located at 960, 1400, 1600, and 3060 cm^{-1} (peaks ii) are not present in the polymer spectrum, and furthermore, there is a rise in the bands at 2870 and 2920 cm^{-1} corresponding to the C-H stretching in aliphatic polyethylene backbone structures (region i) formed during the polymerization of V4D4.[39] It is important to note that PECVD, typically, grows polymer films by random radicalization of the precursor monomer, leading to random recombination reactions and cross-linking between cleaved moieties.[42] This contrasts with targeted deposition methods such as iCVD, which promote film growth by radicalizing more labile bonds such as vinyl groups. Nevertheless, it can be seen from the IR spectra that the use of a lower plasma power promotes the chain growth through the vinyl bonds.

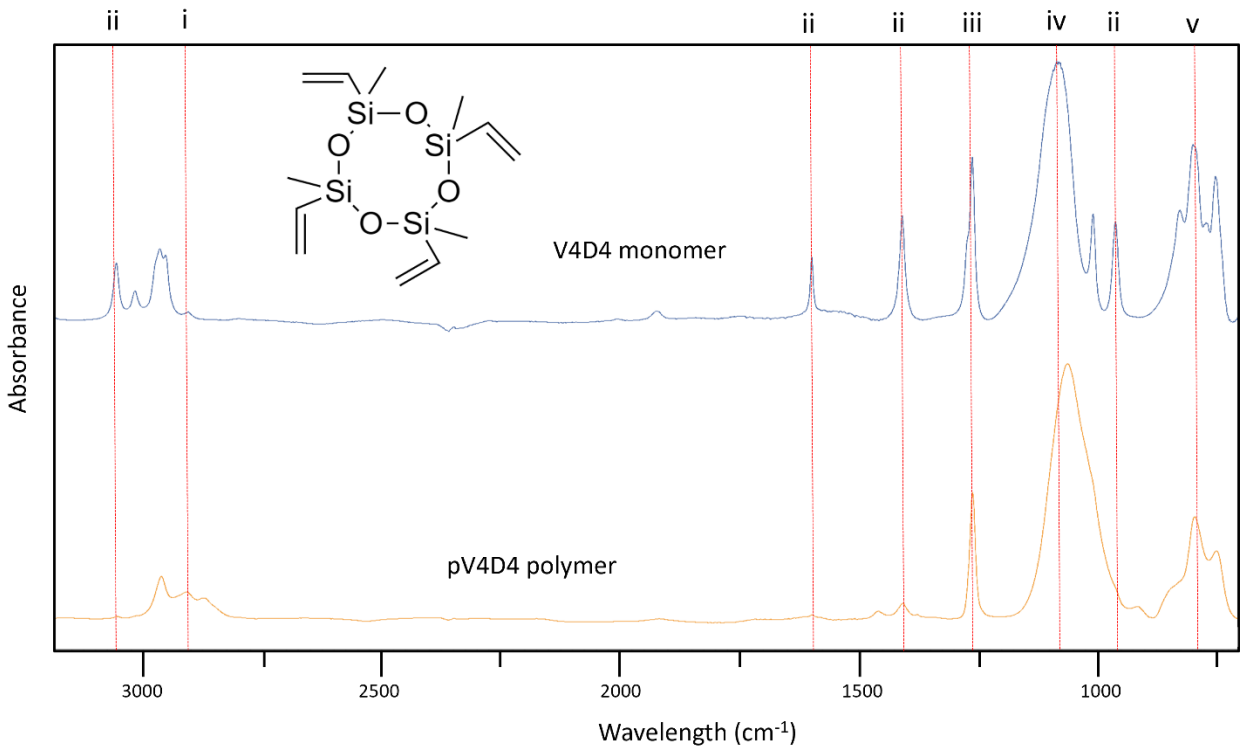

Figure 2: Spectra of the V4D4 monomer and the pV4D4 polymer deposited via PECVD on a Si wafer

We have used FTIR, ex-situ, to characterize the structure of polymer films pyrolyzed at different temperatures. As noted in Section 2.2, Si wafers, chosen due to their high IR transmittance, were used as the substrates to deposit dense, 3 µm thick pV4D4 polymer films using PECVD. The polymer-coated Si wafers were then pyrolyzed as described in Section 2.2. The IR spectra of the pyrolyzed films were immediately collected using transmission FTIR. Figure 3 shows the FTIR spectra of the as deposited pV4D4 film as well as of the polymer films pyrolyzed at different temperatures. Figure 3a shows the FTIR spectra extending from 400 to 3100 cm^{-1}, and Figure 3b and Figure 3c show the expanded views of the regions of the spectra corresponding to the polyethylene and methyl bands, respectively.

FTIR analysis of the pV4D4 sample pyrolyzed at 300 °C shows no significant difference in the peak intensity from the as-deposited pV4D4 sample, thus indicating very little change in its chemical structure. By a pyrolysis temperature of 400 °C, the peaks at 2860 cm^{-1} and 2920 cm^{-1}, corresponding to the C-H in -CH_2-CH_2- backbone bonds (region i), are slightly reduced, due to the cleavage of some of the polyethylene bonds. The methyl stretching bands (region iii), on the other

hand, remain intact at 400 °C with none of the related peaks in Figures 3b and 3c being reduced. The band at 1065 cm^{-1} (SiO_2R_2) still predominates the structure, but bands at 1028 cm^{-1} (Si-O-Si) and 1120 cm^{-1} (SiO_3R, silsesquioxane cage structure) are also present.[1]

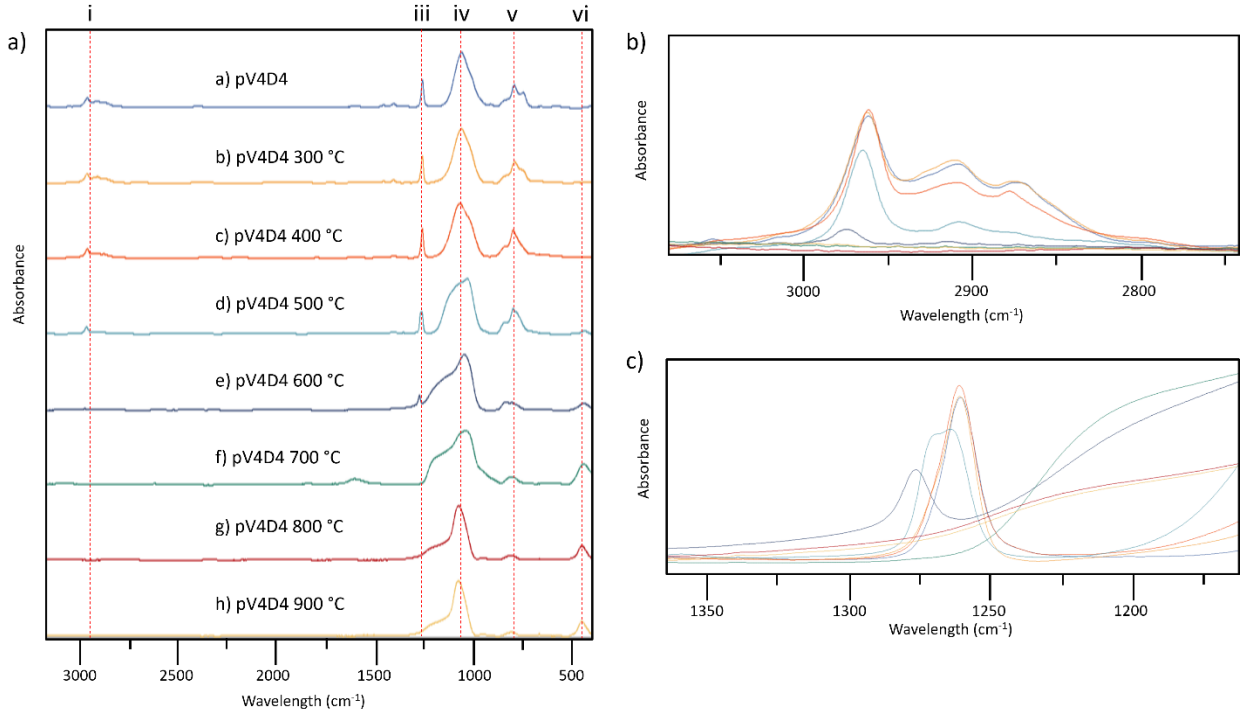

Figure 3: a) Ex-situ IR absorbance spectra showing the transformation of the PECVD-deposited pV4D4 polymer during pyrolysis; b) expanded view of the IR region from 2750 to 3100 cm^{-1} showing the polyethylene stretching band; c) expanded view of the IR region from 1200 to 1300 cm^{-1} showing the methyl stretching band.

This is probably due to the fact that the pyrolysis of pV4D4 was carried out in an inert environment, with fewer oxygen atoms being available to enable the network rings to form silsesquioxane cages. At a pyrolysis temperature of 500 °C, the ethylene peaks at 2860 and 2920 cm^{-1} (region i) are significantly reduced, but the neighbouring methyl peak is only slightly reduced. Furthermore, the Si-CH_3 stretching band transitions from a single peak at 1260 cm^{-1} into a peak doublet at 1262 cm^{-1} and 1275 cm^{-1}. We have previously shown that the splitting of this peak relates to the formation of some silsesquioxane (SiO_3R) groups.[1] The spectra of the pV4D4 sample pyrolyzed at 600 °C shows a broad band between 950 cm^{-1} and 1250 cm^{-1} (region iv), indicating the presence of a mixture of Si-O-Si, silsesquioxane, and Si-O-C bonds.[43] There is also a peak between 400 cm^{-1}

and 500 cm^{-1} (region v) that represents the Si-O-Si out-of-plane deformation typically found in silica structures. [44] By this temperature, the polyethylene bands at 2860 cm^{-1} and 2920 cm^{-1} (region i) have disappeared; the methyl band (region iii) has also been significantly reduced, and has also shifted to a wavelength of 1275 cm^{-1}, indicating that the pyrolyzed polymer has more of a silsesquioxane rather than a network-type structure. At a pyrolysis temperature of 700 °C, the methyl peak has completely disappeared, but the broad band at 1150 cm^{-1} (region iv), likely indicating the presence of Si-O-C in the structure, still remains. At 800 °C, the Si-O-Si band (region iv) continued to change into a silica structure, as indicated by a peak shift to 1065 cm^{-1}, whereas the silsesquioxane and Si-O-C shoulders were significantly reduced. There is no significant change happening in the structure when going from 800 °C to 900 °C, indicating that the polymer has largely finished pyrolyzing by 800 °C.

4.2 pV4D4 Pyrolysis Studied with the Integrated DRIFTS-RGA system

For these experiments, pV4D4 films with a thickness of 10 μm were deposited on BaF_2 powder via PECVD and the resulting polymer-coated powders were then placed inside the cell compartment of the DRIFTS instrument, which was connected with a MS analysis system (RGA). The pV4D4 polymer films were then pyrolyzed in situ by raising the sample temperature (up to 900 °C) in a linear fashion (10 °C/min) with the DRIFTS instrument used to monitor the IR spectra of the films during pyrolysis and the RGA employed for monitoring various gaseous species evolved.

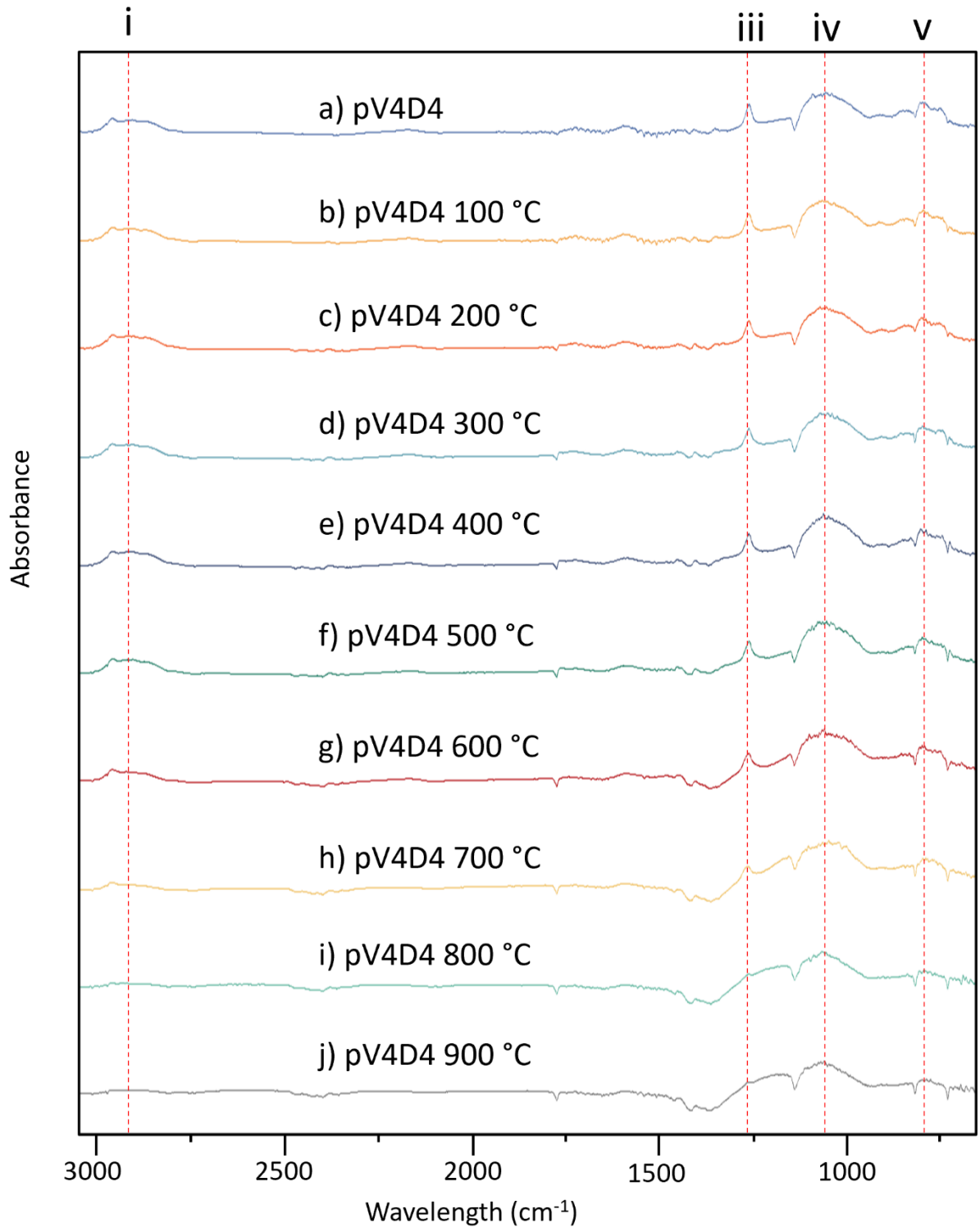

Figure 4: DRIFTS data showing the IR absorbance spectra for pV4D4 films at different pyrolysis temperatures

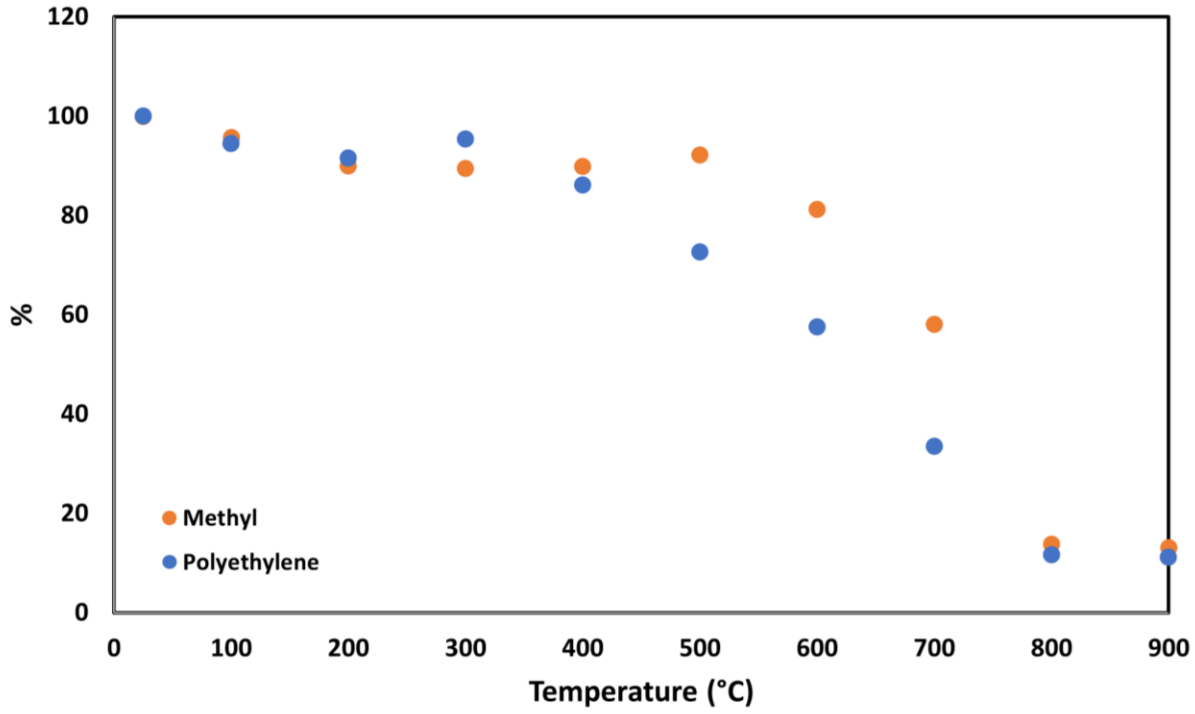

Figure 5: Functional group peak area change as a function of pyrolysis temperature

Figure 4 shows the DRIFTS-IR spectra for the pV4D4 polymer as it undergoes pyrolysis at various temperatures (see Table 1 for the functional groups corresponding to the various major IR bands) and Figure 5 shows the change in the DRIFTS spectra peak area for the polyethylene and methyl bonds. The DRIFTS spectrum of the as-deposited polymer has, as expected, bands that are similar with those found in the FTIR spectrum of the pV4D4 polymer grown on the Si wafer, see Figure 3: A broad band between 950 cm^{-1} and 1100 cm^{-1} that corresponds to the asymmetric Si-O-Si stretching (region iv),[45,46,47], a sharp, prominent band at approximately 1250 cm^{-1} to 1270 cm^{-1} that corresponds to the Si-CH_3 band (region iii), C-H stretching bands between 2800 cm^{-1} and 3000 cm^{-1} corresponding to the polyethylene backbone formed during the polymerization and the CH_3 group (region i), and two small bands in the region between 700 cm^{-1} and 800 cm^{-1} corresponding to the Si-C bending and rocking modes (region v).

As the pyrolysis temperature increased, we found that there were only minimal changes in the IR spectra until a temperature of 400 °C was reached, which is similar to the behavior of the pV4D4 on Si wafers samples pyrolyzed in a tube-furnace (Figure 3). Most notably, the areas the polyethylene backbone (region i) and methyl group (region iii) bands did not noticeably decrease, see Figure 5, which indicates that the pV4D4 chemical structure stayed largely intact up to that

pyrolysis temperature; this observation is in line with the discoveries of other researchers investigating polysiloxane polymer pyrolysis using similar techniques.[48] By 500 °C, there was a small reduction in the polyethylene stretching (region i) and the methyl (region iii) peaks. As the pyrolysis temperature increased past 500 °C, as Figure 5 shows, there was a significant drop in the polyethylene peak area, but this was not the case with the methyl peak. There was, however, a decrease in the methyl band area beginning around 600 °C (Figure 5), which agrees with the observation by Narisawa[49], who found that polysiloxanes had their methyl groups removed at ~600 °C. Both the methyl and the polyethylene peak areas have decreased appreciably by a temperature of 700 °C, and the area of the Si-C bending and rocking peaks (region v) has been largely reduced by this temperature as well. By a pyrolysis temperature of 800 °C, most of the peaks corresponding to the hydrocarbon bonds (regions i, iii, and v) have largely disappeared from the spectra, with the peaks corresponding to Si-O-Si, at around 1050 cm^{-1} and 600 cm^{-1} being the only peak remaining. These are the characteristic IR peaks for amorphous silica.[43] Increasing the pyrolysis temperature to 900 °C did not significantly change the DRIFTS spectra, as the majority of the functional groups have already been cleaved by then. The DRIFTS results with the pV4D4-coated BaF_2 powders are very similar to the observations made with the polymer samples coated on Si wafers and pyrolyzed in a tube-furnace. This shows that the substrate on which these polymer films are deposited has little impact on their structure, and also that the pyrolysis conditions in the DRIFTS chamber resemble those in a conventional tube-furnace.

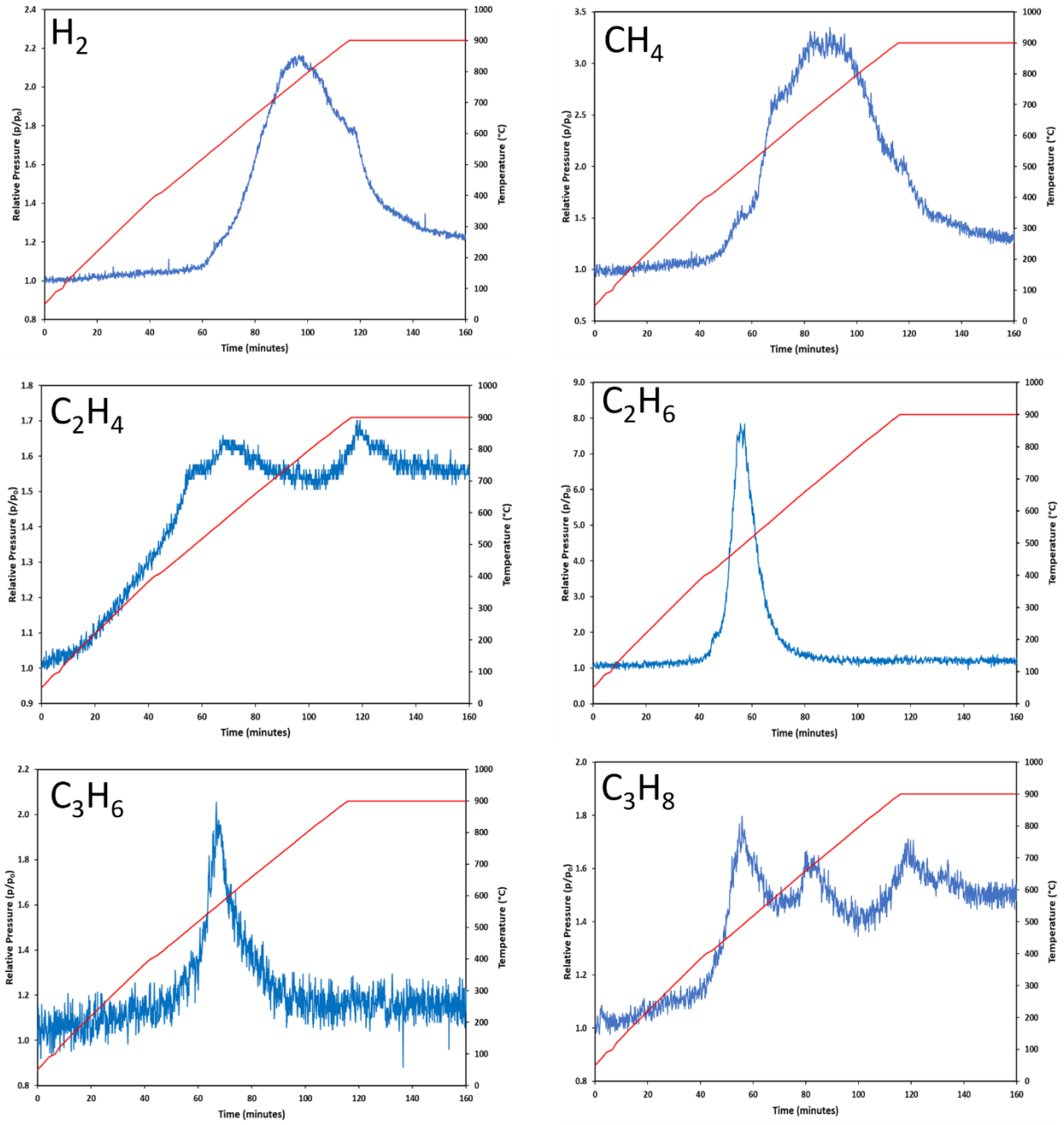

Figure 6: Partial pressures of gaseous species as detected by RGA

During pV4D4 pyrolysis, the RGA instrument attached to the DRIFTS chamber detected several gas phase species, including hydrogen (H_2), methane (CH_4), ethylene (C_2H_4), ethane (C_2H_6), propene (C_3H_6), and propane (C_3H_8), which were emitted from the polymer being pyrolyzed. The increases in the gas phase species concentration detected by the RGA are shown in Figure 6 in terms of the ratio of the partial pressure of the species P measured by the MS detector

divided by the partial pressure P_0 of the same species detected prior to the start of the pyrolysis. It can be seen from the results presented in Figure 6 that gas species evolution primarily took place in two temperature ranges, namely between 400 °C and 500 °C and in between 600 °C and 700 °C. In the first stage of gas species evolution, we observed a large increase in the partial pressure for C_2H_4, C_2H_6, and C_3H_8. The partial pressures for C_2H_6 and C_3H_8 increase sharply, peaking at ~500 °C, and they quickly diminish by the time the pyrolysis temperature has reached 600 °C. Plawsky et. al[50] reported that, during the pyrolysis of an organo-silicate polymer, C_2H_6 is thermodynamically favored to form at temperatures lower than 600 °C, and it is likely generated from free CH_3 radicals recombining. This first stage of gas phase species evolution is associated with the scissioning and loss of the polyethylene polymer backbone due to pyrolysis, as can also be seen in the DRIFTS and ex-situ FTIR spectra. In previous models of polysiloxane polymer pyrolysis[49], it has been seen that the scissioning of -CH_2-CH_2- in the polymer backbone leads to the formation of C_2H_4. Wilson et. al[47,51] also found via MS analysis that during the pyrolysis of polysiloxane polymers, C_2H_4 species were detected at temperatures between 400 °C and 650 °C. In our experiments (Figure 6) in comparison to C_2H_6 and C_3H_8, the increase in C_2H_4 gas phase concentration is more gradual with C_2H_4 being emitted in the gas phase starting with a temperature of 200 °C and its concentration remaining relatively constant throughout the whole pyrolysis experiment. This is indicative that ethylene is continually being formed not only due to reformation of the -CH_2-CH_2- groups but also by the removal and recombination of methyl groups followed by atomic hydrogen abstraction.

The second stage involves the evolution of H_2 and CH_4 (in addition to the constant evolution of C_2H_4 that continues from the first stage) The increase in partial pressure for CH_4 commenced at a temperature of ~425 °C and peaks at a time when the temperature is around 650-700 °C. Such CH_4 evolution behavior has been reported in other MS studies of polysiloxane polymer pyrolysis[47,52] and has been attributed to the homolytic cleavage of Si-CH_3 bonds at elevated temperatures. This is also consistent with the DRIFTS data presented in Figures 4 and 5 that indicate the loss of methyl groups in the same range of temperatures.

The increase in H_2 partial pressure commences at a temperature of ~ 500 ºC and peaks at a temperature of ~750 ºC. During their study of the pyrolysis of polysiloxane gels, Bahloul-Hourlier et. al[51] found that increase in the rate of evolution of CH_4 and H_2 species at these temperatures was

attributed to the formation Si-CH_2-Si and Si-CH_2-CH_2-Si hydrocarbon bridges and their subsequent decomposition. The delayed H_2 evolution is in contrast with lower temperature H_2 evolution observed with other Si-type materials[51], and can be attributed to the lack of Si-H bonds in the pV4D4 polymer. The higher temperature H_2 evolution, which peaks around 750 °C in Figure 6, was previously reported[47,49,50] and was attributed to the scission of C-H bonds which are, typically, the second strongest bonds in siloxane-type polymers after the Si-O bonds, and are known to be cleaved only at temperatures above 600 °C.[49]. The cleavage and recombination of methyl radicals, followed by atomic hydrogen abstraction, is likely responsible for the secondary peak observed during ethylene evolution, see Figure 6.

While the formation of larger molecules such as C_4H_{10} and C_6H_6 are thermodynamically favored during pyrolysis, they were not detected by the RGA in our study. We hypothesize this to be due to the slow diffusion of -CH_2-CH_2- groups in the solid state that kinetically limits the ability of the cleaved polyethylene fragments to recombine into larger MW alkane or cyclic molecules.

4.3 TGA Study of pV4D4 Pyrolysis

TGA was also used to measure the mass loss of the pV4D4 polymer during pyrolysis as a function of time (and corresponding temperature). The mass loss data are complementary to the FTIR and RGA results in the effort to better delineate the mechanism of pV4D4 pyrolysis. For the TGA experiments, as with the DRIFTS/RGA experiments, we utilized BaF_2 powders coated with 5 μm of pV4D4. Prior to using the polymer-coated powder for the TGA experiments, it was dried at 100 °C in a tube-furnace for 1 h under flowing Ar to remove any residual moisture. The experimental heating protocol for the TGA experiments consisted of raising the sample temperature in a linear fashion (3 °C/min) to 100 °C and letting the sample stand (soak) at this temperature for 1 h to remove potential volatile contaminants, including moisture. Subsequently, the sample temperature was raised linearly to 900 °C.[53] We carried out three TGA runs at different heating rates of 5, 10, and 15 K/min in order to determine the effect of heating rate, if any, on the observed behavior.

The mass loss behavior of the pV4D4 polymer can be quantified via the fraction of decomposition (α) defined by Equation 1 below, where m_i, m_t, and m_f are the initial mass, mass at time t, and final mass of the sample, respectively.

$$\alpha = \frac{m_i - m_t}{m_i - m_f} \qquad (1)$$

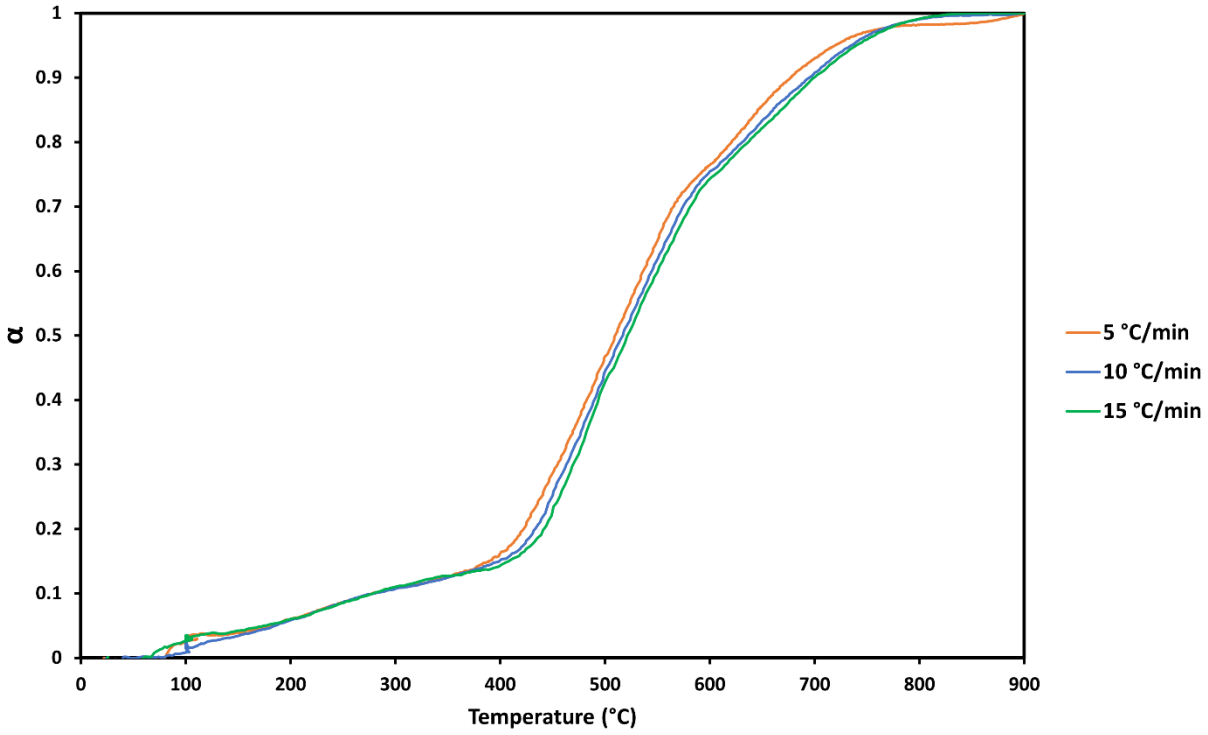

Figure 7: Fraction of decomposition versus temperature for three different heating rates

Figure 7 shows the change in α as a function of temperature for the three different heating rates. Before a temperature of 400 °C, there was a gradual increase of α (with no difference observed between the three heating rates) up to a value of 0.15. This is, likely, due to evolution of small amounts of Si-H, and small amounts of ethylene groups being cleaved off, as also indicated by the RGA results. For temperatures between 400 °C and 700 °C, α increased from 0.15 to 0.9, indicating that this is the range where most of the polymer decomposition occurred. This temperature range also corresponds to the temperature range for which the DRIFTS and RGA results indicated that the majority of the polyethylene and methyl groups were evolved from the polymer structure. In

the temperature range between ~385 °C and ~600 °C, α increased in approximately linear fashion for all 3 heating rates, from ~0.15 to ~0.7. This is the temperature range in which the DRIFTS results indicated that most of the decomposition of the polyethylene backbone took place. Past 600 °C and up to a temperature of 765 °C, α continued to increase linearly, albeit at a slower rate, from ~0.7 to ~0.97, the increase corresponding to the loss of methyl groups, as determined by the DRIFTS/RGA results. Past a temperature of 800 °C, α continues to increase but very slightly, indicating that by this temperature, the polymer had largely finished pyrolyzing.

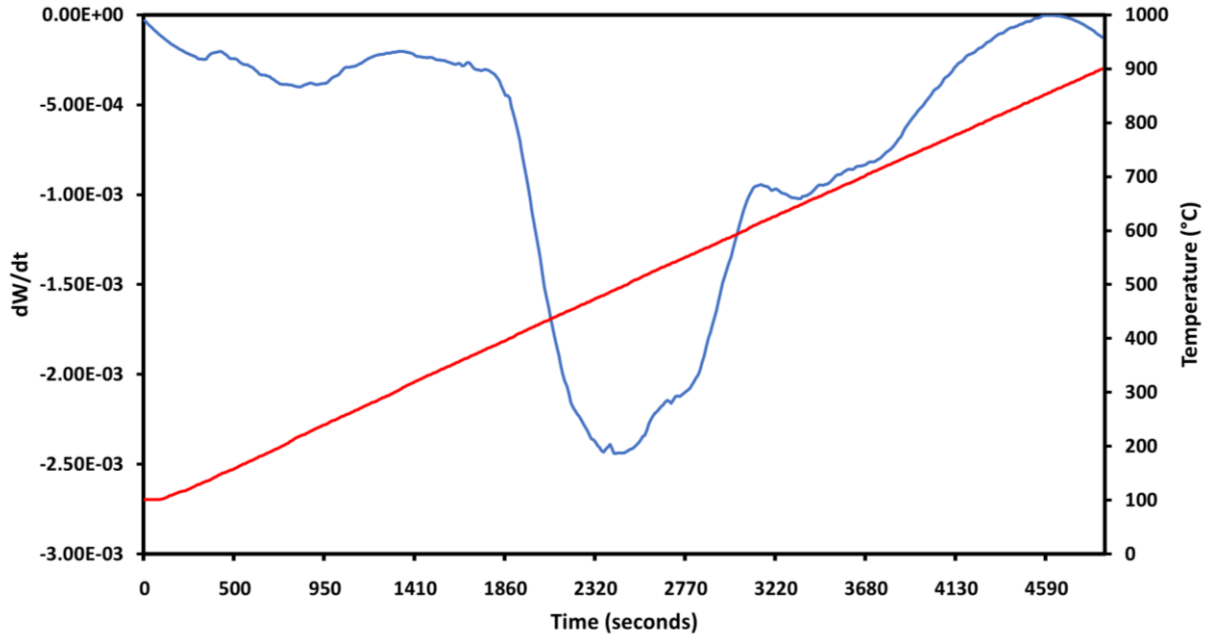

Figure 8: Derivative of weight change during pV4D4 film pyrolysis

To better understand the changes that are occurring in the polymer structure, we calculated the derivative of weight change versus temperature for the 3 K/min heating rate TGA test. The results in Figure 8 indicate the presence of three primary peaks. The first peak, centered around 200 °C, corresponds to very minor scissoning of the polyethylene backbone and methyl groups, as seen in Figure 5. The largest peak, centered around 500 °C, corresponds to the scission of the -CH_2-CH_2- bands from the polyethylene backbone, as also seen in the DRIFTS and ex-situ FTIR results. These reactions contributed to a large mass loss due to the evolution of C_2/C_3 species such as C_2H_4, C_2H_6, and C_3H_8, as shown by the RGA data. The third peak, centered around 700 °C, corresponds to the loss of methyl functional groups from the polymer as well as hydrogen

abstraction from labile C-H bonds. The mass loss corresponding to this peak was smaller in comparison to the larger peak due to the majority of the carbon functional groups from the polyethylene having already been scissioned off the polymer. This small peak correlates to the formation of CH_4 and H_2 species, as also seen by the RGA.

4.4 Atomic Composition Analysis of Materials from pV4D4 Pyrolysis

EDS was used to analyze the atomic composition of the pyrolyzed films. The films were prepared as previously described in Section 4.1. We estimated the electron beam penetration depth to be ~1 μm, so to ensure that there was minimal effect on the EDS results from the Si wafer substrate, the thicknesses of all of the polymer films were measured using a stylus profilometer (AMBiOS XP-2) to ensure they were at least 1.5 μm thick. Prior to the EDS tests, the as prepared films were sputtered with a palladium/platinum coating to increase their conductivity. Table 2 shows the atomic % elemental composition (At%) of the pyrolyzed films from the EDS analysis.

Table 2. At% of the pV4D4 films pyrolyzed at various temperatures

Composition	Deposited	300 °C	400 °C	500 °C	600 °C	700 °C	800 °C	900 °C
C	61.1	57.1	56.1	45.4	29	29.1	3	2.4
O	23.5	23.4	23.5	31.9	45.4	47.7	64.2	67.5
Si	15.4	19.6	20.3	22.7	25.6	23.2	32.8	30.1

For each film, we analyzed three different spots, each at a distance of at least 1 mm apart from the others aiming to determine film uniformity. For each spot, three different measurements were made, and their average values were then compared with those of the other two spots. Good film uniformity was noted. The At% values reported in Table 2 represent the average among the three spots. The results from the EDS experiments are consistent with the observations from the DRIFTS-RGA part of the study (Section 4.2). There is little change in the pyrolyzed film's atomic composition until a major transformation begins to happen between 400 °C and 500 °C. At this temperature, there is a ~10 % reduction in the carbon content of the pyrolyzed pV4D4 film. Between a temperature of 500 °C and 600 °C, there is an additional decrease of ~16 %. These two reductions in the carbon content of the film are, likely, due to the polyethylene -CH_2-CH_2-

functional groups being removed from the structure, as indicated also by the DRIFTS studies (Figures 4 and 5). Between 600 °C and 800 °C, there is a substantial decrease in the carbon content down to 3%. This is consistent with the DRIFTS/RGA results that indicate large shifts in the chemical structure of the film involving the scission of methyl groups from the polymer, the rapid evolution of H_2 and CH_4, and the transition of the polymer into a silica film. Further pyrolysis at a temperature to 900 °C showed negligible changes in the atomic composition of the material, signifying that the transition of the polymer into a silica ceramic was complete by a temperature of 800 °C. Such a conclusion is also supported by the FTIR and DRIFTS observations.

4.6 Computational Studies

The ReaxFF reactive forcefield for pV4D4 was developed by further retuning the parameters[35] from a previous parameterized forcefield for a PDMS polymer system. The ground-truth data-set for this training effort contained the equation of states for bond and angle scans for various configurations, as shown in Figures S1 and S2 in the Supplementary Materials Section. Comparison of ReaxFF and DFT obtained bond and angle scans indicate that the ReaxFF values are in good agreement with the calculated DFT values. DFT calculations were performed using QCHEM code with B3LYP functional with 6-31G** basis set. We trained a total of 49 parameters for this data-set which comprised of two-body, off-diagonal and three-body terms. The two-body C-C, C-Si, O-Si bond terms were reparametrized from the earlier parameterization along with the Si-C and Si-O off-diagonal terms to obtain a good representation of bond-scans with respect to the DFT obtained bond-scan. Further, retuning of the C-Si-C, C-Si-O and O-Si-O three-body angle terms was performed to have an exact representation of the closed ring structure of pV4D4 polymer.

Figure 9 shows the simulation results of the carbon atomic content in the pV4D4 polymer clusters as a function of temperature, expressed as the % fraction of the original number of carbon atoms that still remain in the polymer structure, ATC%, as it is being pyrolyzed. We carried three different pyrolysis simulations that varied from each in the rate (1 K/ps, 2 K/ps, and 3 K/ps) by which we heated up the polymer structure. The differences in behavior among the three simulations is qualitatively similar to the experimental behavior of mass loss (see Figure 7) observed when heating the polymer sample with different heating rates. For all of three simulations, the three

polymer chain structures stayed intact, and the decrease in ATC% was due to the loss of carbon functional groups.

The experimental results discussed above show that as the pyrolysis temperature increased, the carbon At% of the polymer significantly decreased, and the polymer transitioned into a Si-O-C structure. The simulation also showed that as the polymer was heated, starting from a temperature of 300 K, the ATC% also decreased significantly. Interestingly, the number of silicon and oxygen atoms in the polymer structure remained constant, indicating that neither element was removed from the polymer structure during pyrolysis. This is consistent with our RGA studies, in which we did not observe any Si- or O-containing gas phase species. It is, likely, due to the fact that the Si-O bond dissociation energy is known to be significantly higher than the bond dissociation energies for the other bonds found in this siloxane-type polymer.[54,55] Figure 10 shows the mass of the pyrolyzed polymer, expressed as $100X(m/m_0)$, where m is the mass of the polymer at any given time (and corresponding temperature of pyrolysis) and m_0 its initial mass prior to the start of pyrolysis. As expected, the behavior is similar to the one for ATC% in Figure 9.

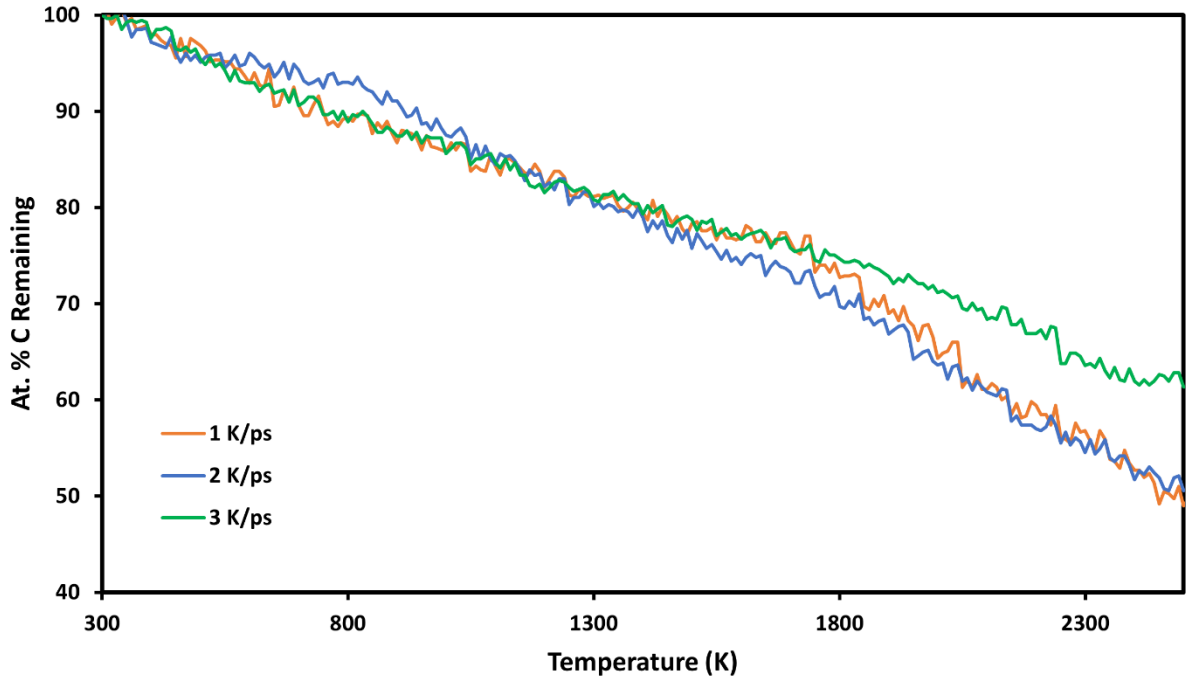

Figure 9: Carbon content of the polymer strands as a function of pyrolysis temperature

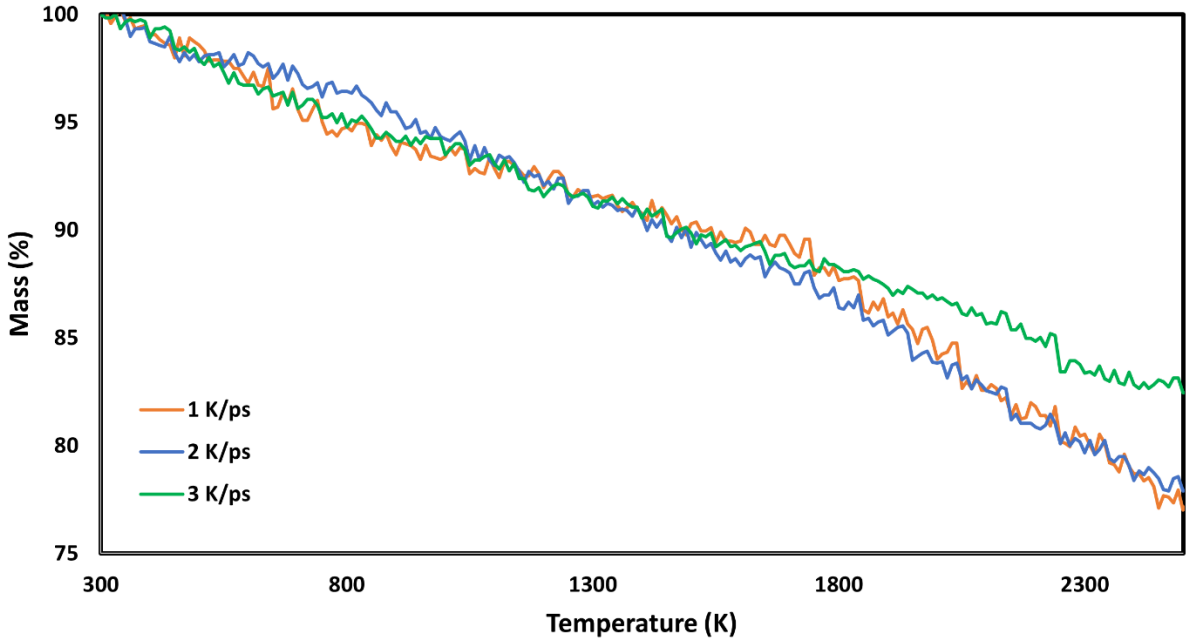

Figure 10: Mass loss of the polymer strands as a function of pyrolysis temperature

In order to better understand the dynamic changes that take place during pyrolysis, in the simulations we "tracked down" the number of Si-C bonds that remain in the simulation box. In Figure 11, we plot the fraction of the original bonds that remain in the polymer structure as it is being pyrolyzed at various temperatures. As the temperature increases past 700 K, there is a steady decrease of the Si-C bonds in the system, which are known to be more labile than the tight cyclic Si-O bonds.[35] Such a decrease is attributed to the disintegration of the polyethylene bands, and also to scissioning of the methyl groups from the polymer.

In the simulations we also tracked down the number of stable gas phase species in the simulation box, which are shown in Figure 12. The simulations indicate the formation of H_2, CH_4, and C_2, C_3 and C_4 hydrocarbon species, all of which (other than the C_4 species) were also observed experimentally, as noted previously. Further, the simulations do not detect the presence of C_5 or C_6 hydrocarbon species, in line with the experimental observations. We attempt no quantitative comparisons here between the simulations and the RGA compositional data, as the experimental set-up is a flow system and the simulations employ a close system. Given such differences, it is quite remarkable that even a good qualitative agreement is attained.

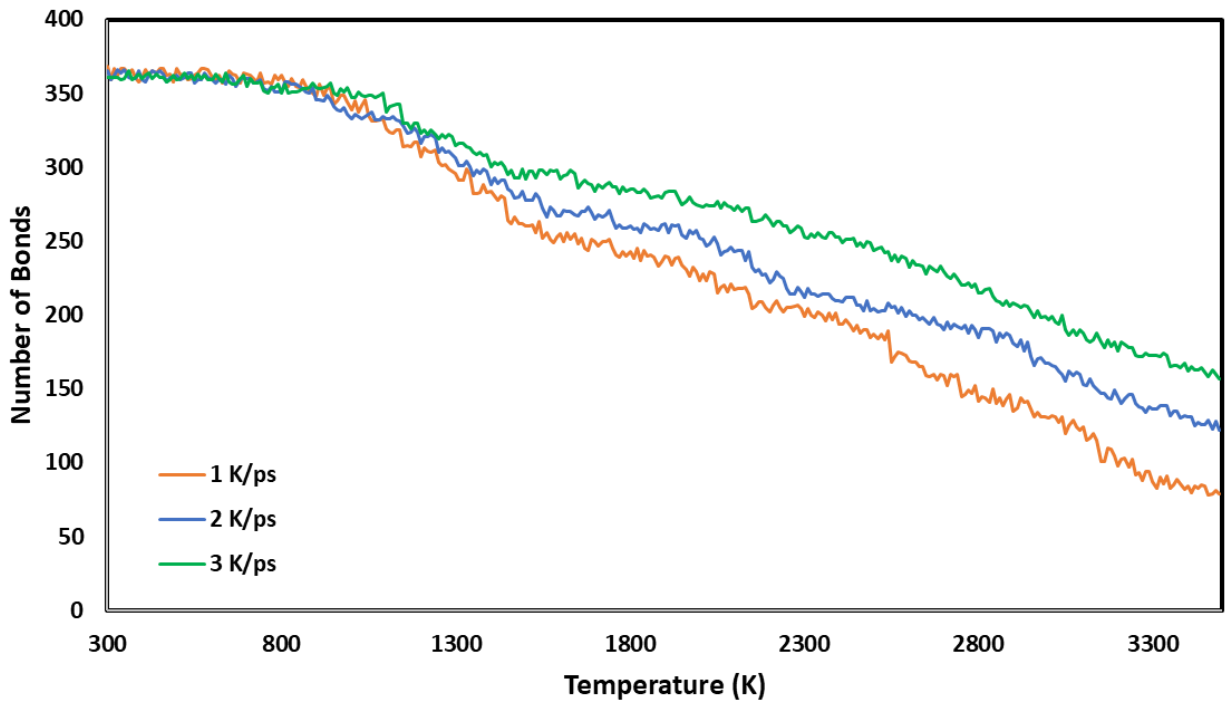

Figure 11: Temperature evolution of the Si-C bonds during the pyrolysis of pV4D4

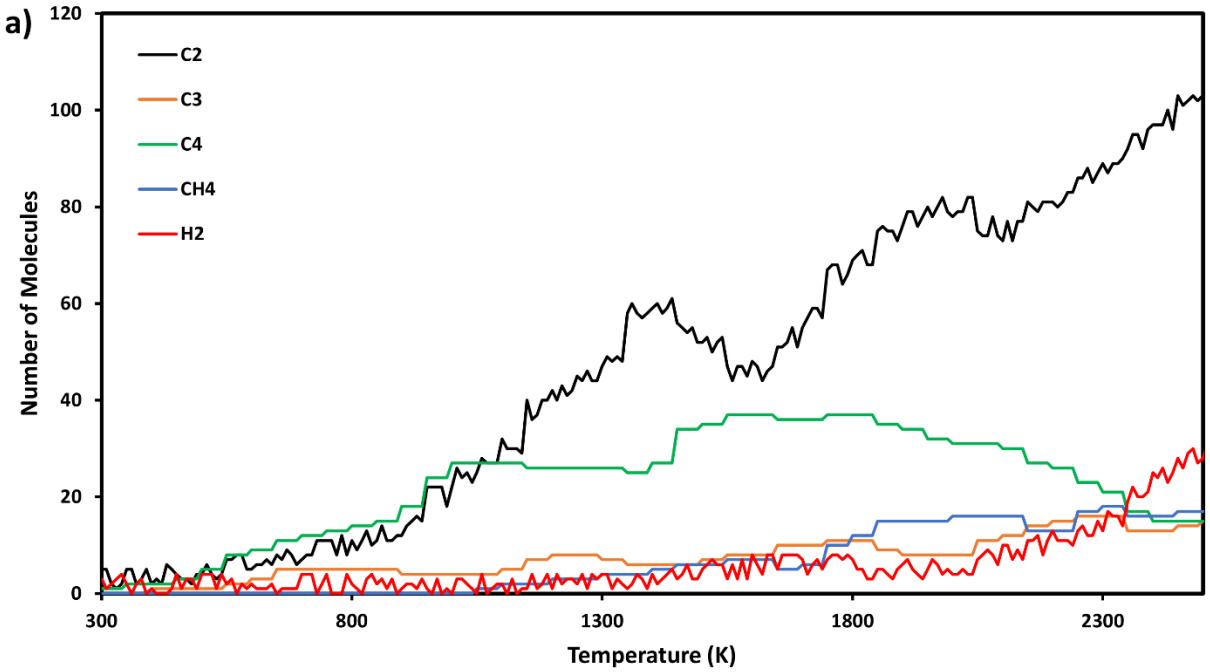
a)
C2
C3
C4
CH4
H2
Number of Molecules
Temperature (K)
0
20
40
60
80
100
120
300
800
1300
1800
2300

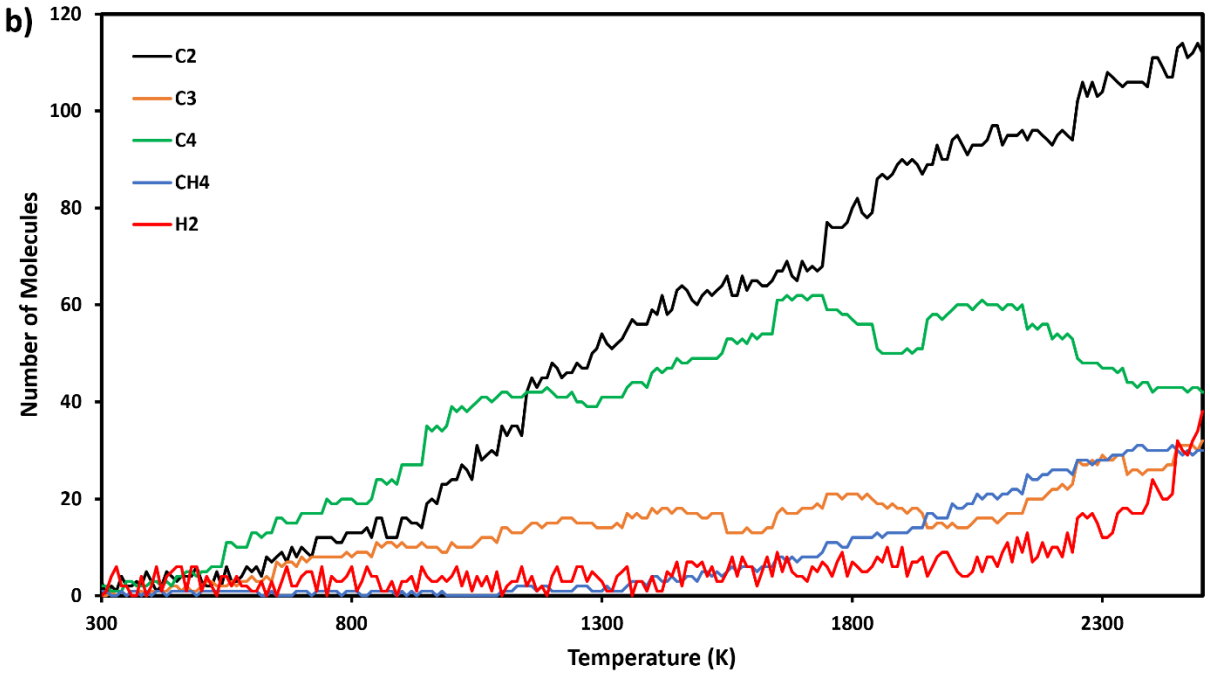
b)
C2
C3
C4
CH4
H2
Number of Molecules
Temperature (K)
0
20
40
60
80
100
120
300
800
1300
1800
2300

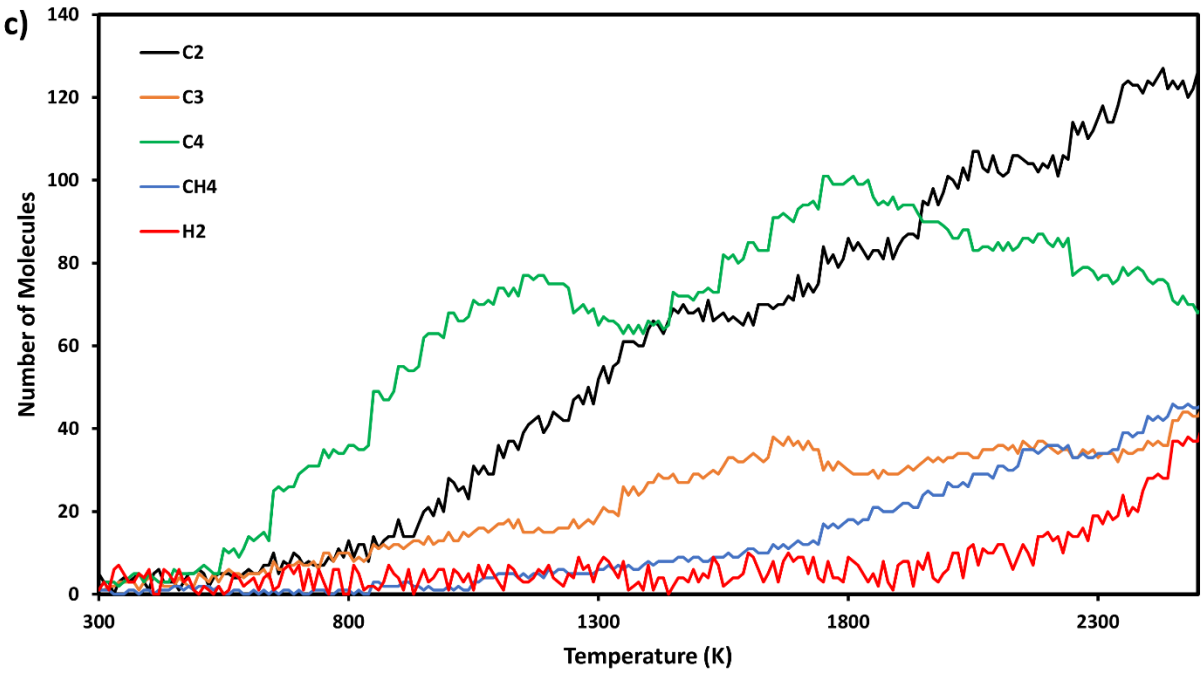

Figure 12: Evolution of the compounds observed during the pyrolysis process for the a) 1 K/ps, b) 2 K/ps, and c) 3 K/ps heating rate simulations.

5. Conclusion

In this study, we developed a methodology to investigate the pyrolysis of a PECVD-deposited pV4D4 film. In situ DRIFTS was used to analyze the changes in the solid-state bonding environment, and time-resolved MS was employed to monitor the concentration of gas phase species evolved as the pV4D4 polymer was being pyrolyzed. Combining these two in situ techniques allowed us to establish that pV4D4 pyrolysis takes place in two distinct stages. The first stage is associated with the cleavage of the more labile polyethylene backbone formed during the polymerization and leads to the release of C_2 and C_3 species such as ethylene and propane. The second stage is associated with the cleavage of the methyl groups, and with hydrogen abstraction from C-H bonds, which then leads to the formation of CH_4 and H_2.

The DRIFTS and time-resolved MS techniques were also complemented with TGA measurements that further helped to confirm the two-stage mechanism of pV4D4 pyrolysis. EDS was used to provide an elemental analysis of the pyrolyzed polymer samples. The EDS results are

in line with the FTIR/DRIFTS measurements and confirm that polymer pyrolysis is complete by a temperature of ~800 °C to form a silica material with a very minor amount of carbon remaining in its structure. A computational model using ReaxFF was developed and utilized to provide further fundamental insight into the molecular processes that lead to the formation of inorganic silica films from siloxane-type, pre-ceramic polymer precursors. Good qualitative agreement between simulations and experiments was found.

6. Acknowledgements

The authors acknowledge the support of the National Science Foundation (Award# CMMI-2012196). The EDS data were acquired at the Core Center of Excellence in Nano-Imaging at the University of Southern California.

---

[1] Nguyen, B., Dabir, S., Tsotsis, T., and Gupta, M. Fabrication of Hydrogen-Selective Silica Membranes via Pyrolysis of Vapor Deposited Polymer Films. Ind. Eng. Chem. Res. 2019, 58, 33, 15190–15198.
[2] Ockwig, N. W. and Nenoff, T. M. Membranes for Hydrogen Separation. Chem. Rev., 2007, 4078–4110.
[3] Elyassi, B., Sahimi, M., and Tsotsis, T. Inorganic Membranes. Encyclopedia of Chemical Processing, 2009, 1–16.
[4] Yi, B., Wang, S., Hou, C., Huang, X., Cui, J., and Yao, X. Dynamic Siloxane Materials: From Molecular Engineering to Emerging Applications, Chem. Eng. J., 2021, 405, 127023.
[5] Fujii, T., Yokoi, T., Hiramatsu, M., and Nawata, M. Low di-electric constant film formation by oxygen-radical polymerization of laser-evaporated siloxane. J. Vac. Sci. Technol. B, 1997, 15, 746.
[6] Qi, H., Wang, X., Zhu, T., Li, J., Xiong, L., and Liu, F. Low Dielectric Poly(imide siloxane) Films Enabled by a Well-Defined Disiloxane-Linked Alkyl Diamine. ACS Omega, 2019, 4, 26, 22143-22151.
[7] Wang, Z., Wang, H., Mitra, A., Huang, L., and Yan, Y. Pure-Silica Zeolite Low-K Dielectric Thin Films, Adv. Mater., 2001, 13, 10, 746-749.
[8] Katagiri, K., Yamazaki, S., Inumaru, K., and Koumoto, K. Anti-reflective coatings prepared via layer-by-layer assembly of mesoporous silica nanoparticles and polyelectrolytes, Polym. J., 2015, 47, 190-194.
[9] Biswas, P. K., Devi, P., Chakraborty, P., Chatterjee, A., Ganguli, D., Kamath, M., and Joshi, A. Porous anti-reflective silica coatings with a spectral coverage by sol-gel spin coating technique, J. Mater. Sci. Lett., 2003, 22, 181-183.
[10] Dowling, D., Nwankire, C., Riihimaki, M., Keiski, R., and Nylen, U. Evaluation of the Anti-fouling Properties of nm Thick atmospheric Plasma Deposited Coatings, Surf. Coat. Technol., 2010, 205, 5, 1544-1551.
[11] Zhang, H., and Chiao, M. Anti-fouling Coatings of Poly(dimethylsiloxane) Devices for Biological and Biomedical Applications, J. Med. Biol. Eng., 2015, 35, 143-155.
[12] Roualdes, S., Sanchez, J., and Durand, J. Gas Diffusion and Sorption Properties of Polysiloxane Membranes Prepared by PECVD, J. Membr. Sci., 2002, 198, 299-310.
[13] Bazmi, M., Tsotsis, T., Jessen, K., Ciora, R., & Parsley, D. Advanced Ceramic Membranes/Modules for Ultra Efficient Hydrogen (H_2) Production/Carbon Dioxide (CO_2) Capture for Coal-Based Polygeneration Plants: Fabrication, Testing, and CFD Modeling. Media and Process Technology Inc. 2022, doi:10.2172/1895357.
[14] Hall, D.B., Underhill, P., and Torkelson, J.M. Spin coating of thin and ultrathin polymer films, Polym. Eng. Sci., 1998, 38, 12, 2039-2045.
[15] Saputra, R.E., Astuti, Y., and Darmawan, A. Hydrophobicity of silica thin films: The deconvolution and interpretation by Fourier-transform infrared spectroscopy, Spectrochimica Acta Part A: Molecular and Biomolecular Spectroscopy, 2018, 199, 12-20.

[16] Boffa, V., Blank, D.H., and ten Elshof, J.E. Hydrothermal stability of microporous silica and niobia–silica membranes, J. Membr. Sci., 2008. 319, 1-2, 256-263.
[17] Iarikov, D.D., P. Hacarlioglu, and S.T. Oyama, Amorphous silica membranes for H2 separation prepared by chemical vapor deposition on hollow fiber supports, in Membrane Science and Technology, 2011, Elsevier, 61-77.
[18] Khatib, S.J. and S.T. Oyama, Silica membranes for hydrogen separation prepared by chemical vapor deposition (CVD), Sep. Purif. Technol., 2013, 111, 20-42.
[19] Gleason, K.K., CVD polymers: fabrication of organic surfaces and devices, 2015, John Wiley & Sons.
[20] Ozaydin-Ince, G., Coclite, A.M., and Gleason, K.K. CVD of polymeric thin films: applications in sensors, biotechnology, microelectronics/organic electronics, microfluidics, MEMS, composites and membranes, Reports on Progress in Physics, 2011, 75, 1, 016501.
[21] Coclite, A.M., et al., 25th Anniversary article: CVD polymers: a new paradigm for surface modification and device fabrication. Adv. Mater., 2013, 25, 38, 5392-5423.
[22] Gleason, K.K. Overview of chemically vapor deposited (CVD) polymers, CVD Polymers: Fabrication of Organic Surfaces and Devices, 2015, 1-11.
[23] de Freitas, A.S., et al., Organosilicon films deposited in low-pressure plasma from hexamethyldisiloxane—A review, Vacuum, 2021, 194, 110556.
[24] Sreenivasan, R. and Gleason, K. K. Overview of Strategies for the CVD of Organic Films and Functional Polymer Layers, Chem. Vap. Deposition, 2009, 15, 77-90.
[25] Chen, N., Kim, D. H., Kovacik, P., Sojoudi, H., Annu. Rev. Chem. Biomol. Eng. 2016, 7, 373.
[26] Shen, B., Wang, S., and Tenhaeff, W. Ultrathin Conformal Polycyclosiloxane Films to Improve Silicon Cycling Stability, Science Advances, 2019, 5, 7.
[27] Larkin, P. Chapter 3 - Instrumentation and Sampling Methods, In Infrared and Raman Spectroscopy, 2011, 27-54
[28] Thompson, J. M. Mass spectrometry, 2018, Pan Stanford.
[29] Wang, X., Hong, Y., Shi, H., and Szanyi, J. Kinetic Modeling and Transient DRIFTS-MS Studies of CO_2 Methanation over Ru/Al_2O_3 Catalysts, Journal of Catalysis, 2016, 343, 185-195.
[30] Ochoa, J., Trevisanut, C., Millet, J., Busca, G., and Cavani, F. In Situ DRIFTS-MS Study of the Anaerobic Oxidation of Ethanol over Spinel Mixed Oxides, J. Phys. Chem. C., 2013, 117, 45, 23908-23918.
[31] White, R. Thermal Analysis by Diffuse Reflectance Fourier Transform Infrared Spectroscopy-Mass Spectrometry, J. Anal. Appl. Pyrolysis, 1991, 18, 325-339.
[32] Carlsson, D. J., Cooney, J. D., Gauthier, S., Worsfold, D. J. Pyrolysis of Silicon-Backbone Polymers to Silicon Carbide, Am. Ceram. Soc. 1990, 73, 2, 237–241.
[33] Nomura, K., Kalai, R., Nakano, A., Rajak, P., and Vashista, P. RXMD: A scalable reactive molecular dynamics simulator for optimized time-to-solution., SoftwareX, 2020, 11, 100389.
[34] van Duin, A.C.T, Dasgupta, S., Lorant, F., and Goddard, W. A. ReaxFF: a Reactive Force Field for Hydrocarbons, J. Phys. Chem. A, 2001, 105, 9396-9409.
[35] Naserifar, S., Goddard, W., Liu, L., Tsotsis, T., and Sahimi, M. Toward a Process-Based Molecular Model of SiC Membranes 2. Reactive Dynamics Simulation of the Pyrolysis Precursor to Form Amorphous SiC, J. Phys. Chem. C, 2013, 117, 7, 3320-3329.
[36] Chenoweth, K., Cheung, S., van Duin, A., Goddard, W., and Kober, E. Simulations on the Thermal Decomposition of a Poly(dimethylsiloxane) Polymer Using the ReaxFF Reactive Force Field, J. Am. Chem. Soc., 2005, 127, 19, 7192-7202.
[37] Chen, S., Liu, C., Li, Q., Liu, Y., Xin, L., and Yu, W. A ReaxFF-based Molecular Dynamics Study of the Pyrolysis Mechanism of Hexamethyldisiloxane, J. Mol. Liq., 2002, 356, 119026.
[38] Shao,Y., Gan, Z., Epifanovsky, E., Gilbert, A. T. B., Wormit, M., Kussmann, J., Lange, A. W., Behn, A., Deng, J., Feng, X… and Head-Gordon, M. Advances in molecular quantum chemistry contained in the Q-Chem 4 program package, Mol. Phys., 2015, 113, 184-215.
[39] S. M. Gates, D. A. Neumayer, M. H. Sherwood, A. Grill, X. Wang, M. Sankarapandian, Preparation and structure of porous dielectrics by plasma enhanced chemical vapor deposition. J. Appl. Phys., 2007 101, 094103.
[40] Trujillo, N., Wu, Q., and Gleason, K.K. Ultralow Dielectric Constant Tetravinyltetramethylcyclotetrasiloxane Films Deposited by Initiated Chemical Vapor Deposition (iCVD), Adv. Funct. Mater., 2010, 20, 4, 607-616.
[41] Kherroub, D., Belbachir, M., and Lamouri, S. Activated bentonite (Maghnite-H+) as green catalyst for ring-opening polymerization of 1,3,5,7-tetravinyltetramethylcyclotetrasiloxane, Res. Chem. Intermed., 2017, 43,10.

[42] Hamedani, Yasaman et al. Plasma-Enhanced Chemical Vapor Deposition: Where we are and the Outlook for the Future, Chemical Vapor Deposition - Recent Advances and Applications in Optical, Solar Cells and Solid State Devices, edited by Sudheer Neralla, IntechOpen, 2016.
[43] Oh. T., and Choi, C. Comparison between SiOC Thin Films Fabricated by Using Plasma Enhanced Vapor Deposition and SiO2 Thin Films by Using Fourier Transform Infrared Spectroscopy, J. Korean Phys. Soc., 2010, 56, 4, 1150-1155.
[44] Ellerbrock, R., Stein, M., and Schaller, J. Comparing amorphous silica, short-range-ordered silicates and silicic acid species by FTIR. Sci Rep., 2022, 12, 11708.
[45] Sassin, M., Long, J., Wallace, J., and Rolison, D. Routes to 3D conformal solid-state dielectric polymers: electrodeposition versus initiated chemical vapor deposition, Mater. Horiz., 2015, 2, 502.
[46] Choi, J., Seong, H., Pak, K., and Im., S. Vapor-phase deposition of the fluorinated copolymer gate insulator for the p-type organic thin-film transistor, J. Inf. Disp., 2016, 17, 2, 43-49.
[47] Ondo, D., Loyer, F., Werner, F., Leturcq, R., Dale, P., and Boscher, N. Atmospheric-Pressure Synthesis of Atomically Smooth, Conformal, and Ultrathin Low-k Polymer Insulating Layers by Plasma-Initiated Chemical Vapor Deposition, ACS Appl. Polym. Mater., 2019, 1, 3304-3312.
[48] Wilson, A., Zank, G., Eguchi, K., Xing, W., Yates, B., and Dahn, J. Polysiloxane Pyrolysis, Chem. Mater., 1997, 9, 1601-1606.
[49] Narisawa, M. Silicone Resin Applications for Ceramic Precursors and Composites. Mater., 2010, 3 (6), 3518–3536.
[50] Plawsky, J., Wang, F., and Gill, W. Kinetic Model for the Pyrolysis of Polysiloxane Polymer to Ceramic Composites, AIChe J., 2002, 481, 10, 2315-2323.
[51] Wilson, A.M., Zank, G., Eguchi, K., Xing, W., Yates, B., and Dahn, J.R., Pore Creation in Silicon Oxycarbides by Rinsing in Dilute Hydrofluoric Acid, Chem. Mater., 1997, 9, 2139-2144.
[52] Bahloul-Hourlier, D., Latournerie, J., Dempsey, P. Reaction Pathways During the Thermal Conversion of Polysiloxane Precursors into Oxycarbide Ceramics, J. Eur. Ceram. Soc., 2005, 25, 979-985.
[53] Tabarkhoon, F., Abolghasemi, H., Rashidi, A., Bazmi, M., Alivand, M.S., Tabarkhoon, F., Farahani, M.V. and Esrafili, M.D. Synthesis of Novel and Tunable Micro-Mesoporous Carbon Nitrides for Ultra-High CO_2 and H_2S capture. Chemical Engineering Journal., 2023, 456, p.140973.
[54] Walsh, R. Bond Dissociation Energy Values in Silicon-Containing Compounds and Some of Their Implications, Acc. Chem. Res., 1981, 14, 246-252.
[55] J. Dean (Eds.). Lange's Handbook of Chemistry. McGraw-Hill, New York, 14th edition, (1992)

Supplementary Section

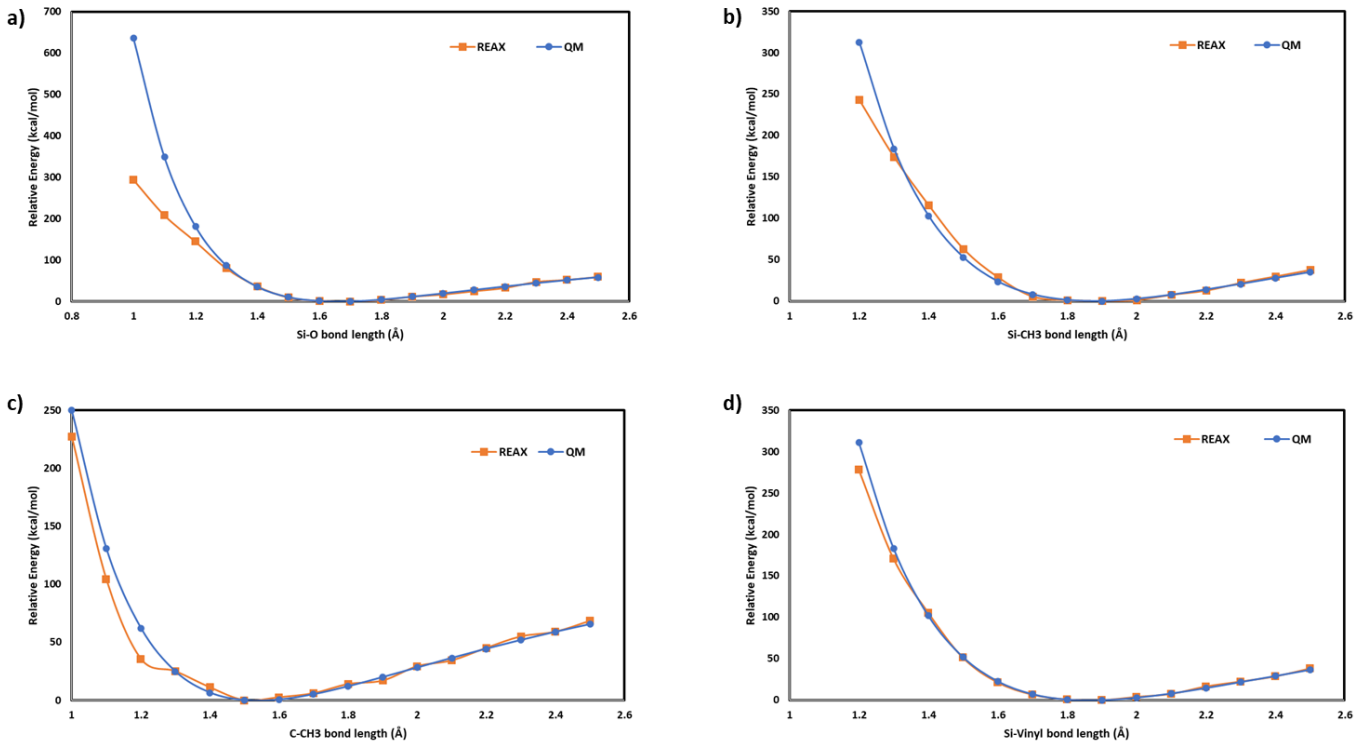

Figure S1: Comparison of the ReaxFF and DFT bond dissociation energies for the following bonds: a) Si-O, b) Si-CH3, c) C-CH3, and d) Si-Vinyl.

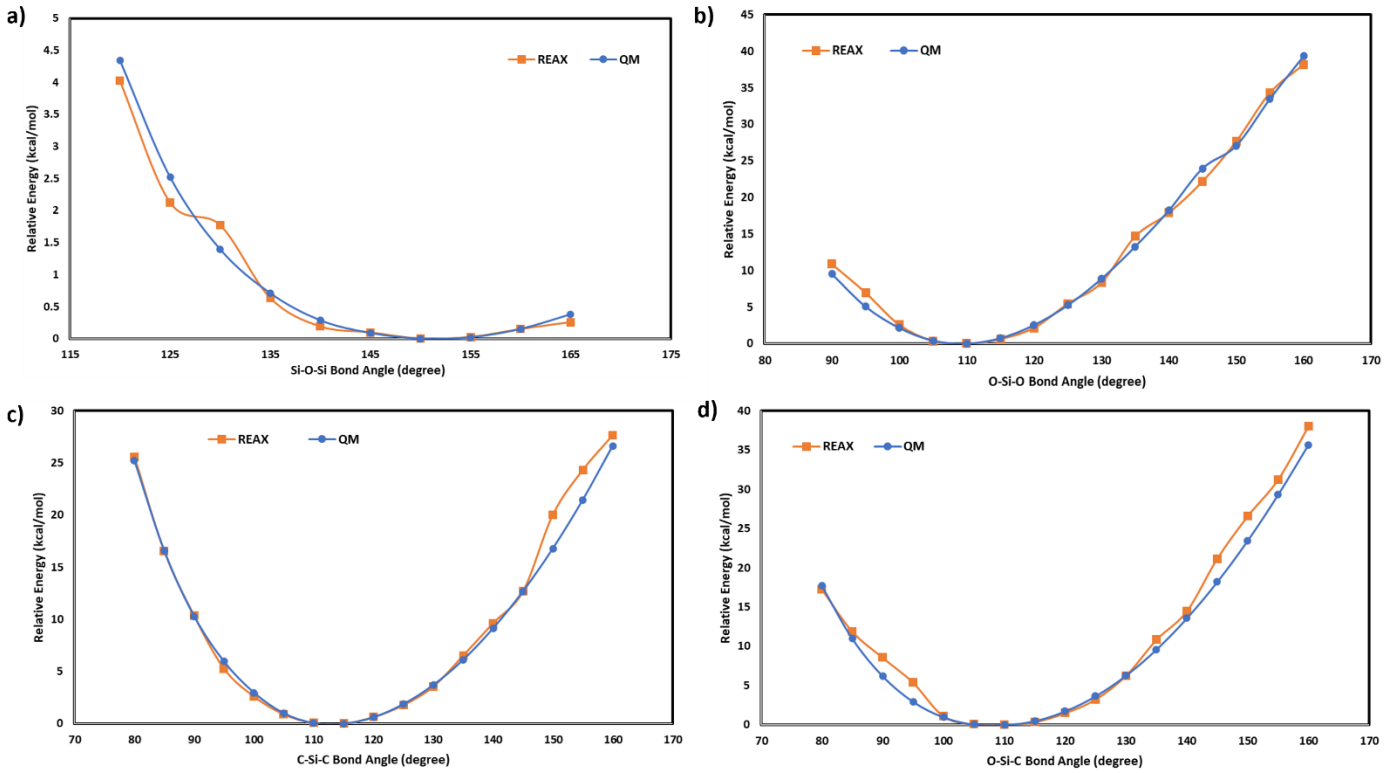

Figure S2. Comparison of the ReaxFF and DFT bond angle distortion energies for the following bonds: a) Si-O-Si, b) O-Si-O, c) C-Si-C, and d) O-Si-C.